Lithospheric structure of the Yukon, northern Canadian Cordillera, obtained from magnetotelluric data

Juanjo Ledo[1] and Alan G. Jones[2]
Geological Survey of Canada, Ottawa, Ontario, Canada

Ian J. Ferguson and Lisa Wolynec
Geological Sciences, University of Manitoba, Winnipeg, Manitoba, Canada

Received 24 March 2003; revised 29 January 2004; accepted 12 February 2004; published 30 April 2004.

[1] Two goals of Lithoprobe's geoscientific studies in the Phanerozoic accretionary cordillera of western North America were to define the subsurface geometries of the terranes and to infer the physical conditions of the crust. These questions were addressed in Canada's southern cordillera a decade ago and have more recently been addressed in the northern cordillera, of which one component of the new studies is magnetotelluric (MT) profiling from ancestral North American rocks to the coast. We present a resistivity cross section, and its interpretation, of the northern cordillera derived from modeling data from 42 MT sites along a 470-km-long NE-SW profile. Beneath the Coast Belt (southwestern end of the profile) a deep crustal low-resistivity layer dips inland; we interpret the crustal part of this conductor as being due to metasedimentary rocks emplaced and metamorphosed during Paleocene Kula plate subduction. A strong lateral transition in lithospheric mantle resistivity exists below the Intermontane Belt that is spatially coincident with changes in chemical and isotopic characteristics of Tertiary to recent alkaline lavas, suggesting that isotopically enriched lithosphere related to the Coast Belt basalts extends partly beneath the Intermontane Belt. The unusually high lower crustal resistivity in the Intermontane and Omineca Belts, similar in value to the resistivity found in the unextended part of central British Columbia, excludes the presence of fluids or conducting metasediments. Finally, our resistivity model displays strong lateral variation of the middle and lower crust between different terranes within the same belt, as a result of the complex structural evolution of the lithosphere. *INDEX TERMS:* 0925 Exploration Geophysics: Magnetic and electrical methods; 1515 Geomagnetism and Paleomagnetism: Geomagnetic induction; 8110 Tectonophysics: Continental tectonics—general (0905); 8120 Tectonophysics: Dynamics of lithosphere and mantle—general; *KEYWORDS:* magnetotelluric, accreted terranes, northern Canadian Cordillera

Citation: Ledo, J., A. G. Jones, I. J. Ferguson, and L. Wolynec (2004), Lithospheric structure of the Yukon, northern Canadian Cordillera, obtained from magnetotelluric data, *J. Geophys. Res.*, *109*, B04410, doi:10.1029/2003JB002516.

1. Introduction

[2] The cordillera of western North America consists of a collage of precordilleran sediments, oceanic and island arc terranes (accreted since the Neoproterozoic) and igneous rocks, with most of the westward growth occurring during the Mesozoic on the long-lived stable western margin of North America. In northern Canada, the tectonic elements have been displaced northward along large dextral strike-slip faults caused by the relative motion between the Pacific Ocean basin and the North American continent. The Canadian Cordillera can broadly be divided into five major physiographic belts generally representing fault zone bounded geological units of regional extent. With the exception of the easternmost Foreland Belt, each belt comprises a collection of different allochthonous terranes, and each terrane is characterized by its own unique geological and tectonic history distinctly different from its neighbors. Within the multidisciplinary Lithoprobe program (Canada's National Geoscience Project) [*Clowes et al.*, 1992, 1998] the Slave-Northern Cordillera Lithospheric Evolution (SNORCLE) transect is aimed at unraveling the complex interrelationships between the terranes, and determining the subsurface nature of the terrane boundaries and their physical states. To address these themes, a magnetotelluric (MT) experiment was conducted in the northern cordillera during the summer and fall of 1999, and included three regional-scale profiles, which crossed the main geological structures, and a high-resolution profile crossing the Tintina Fault [*Ledo et al.*, 2002a]. In this paper we present

[1]Now at Departament de Geodinamica i Geofisica, Universitat de Barcelona, Barcelona, Spain.
[2]Now at Dublin Institute for Advanced Studies, Dublin, Ireland.

0148-0227/04/2003JB002516$09.00

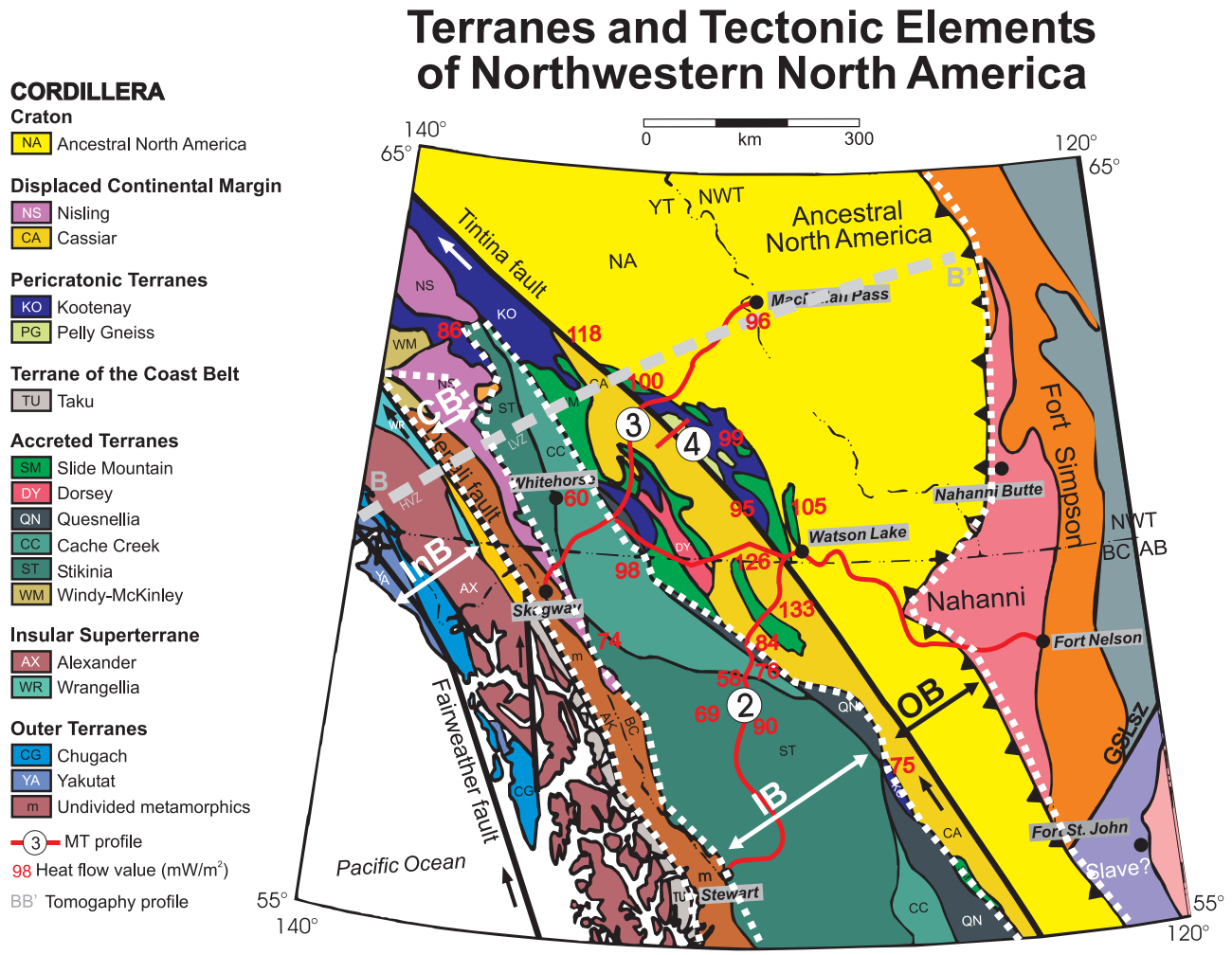

Figure 1. Terranes and belts map of the northern Canadian Cordillera. Red lines, MT profiles; red values, heat flow data (mW/m^2); BB′, location of the tomograpic profile used for Figure 9 [Plate 4]. (Modified after P. Erdmer, unpublished data, 1995.)

results from SNORCLE Corridor 3, which is located mainly in the Yukon Territory and extends for 470 km from north of Skagway (Alaska), to the MacMillan Pass at the border between Yukon and the Northwestern Territories (Figures 1 and 2).

[3] The primary objective of the SNORCLE Corridor 3 MT experiment was to determine the electrical resistivity structure of the crust and the upper mantle beneath the Yukon Territory across the accreted terranes and ancestral North America beyond the Tintina Fault. The profile starts in the west within the Coast Belt, continues into the Intermontane Belt, crosses the Teslin Fault, the limit between the Intermontane and Omineca Belts, and, after traversing the intracontinental strike-slip Tintina Fault (TTF), samples the Foreland Belt and Ancestral North America rocks.

[4] In total, 42 broadband MT (BBMT) soundings were acquired along Corridor 3 with a period range of 0.001 (frequency of 1000 Hz) to about 3000 s. In addition, long-period MT data (LMT), with a period range of 20–20,000 s, were acquired at every other BBMT site. The average site spacing was 11.5 km; the maximum separation was 15 km and the minimum distance was 5 km for the sites located close to the TTF. Time series processing employed modern robust methods [*Jones et al.*, 1989]. Subsequently, MT tensor decomposition techniques [*Groom and Bailey*, 1989; *McNeice and Jones*, 2001] were used on the impedance tensor estimates to identify and remove distortions caused by local near-surface features and to derive the regional two-dimensional (2-D) MT impedances in the most appropriate geoelectric strike directions. Finally, a regional-scale 2-D resistivity model of the regional responses was derived through the nonlinear conjugate gradients inversion algorithm of *Rodi and Mackie* [2001]. In this paper we describe those steps, and we compare our derived resistivity model with other geophysical and geological data, and draw inferences from it about the physical state of the crust and upper mantle.

2. Geological and Geophysical Data

[5] The Canadian Cordillera is an orogenic collage, the aftermath of superimposed systems of subduction, seafloor spreading and transform faulting; an example of orogenic collage that is forming today is Indonesia [*Monger and Price*, 2002]. During Jurassic and Early Cretaceous times,

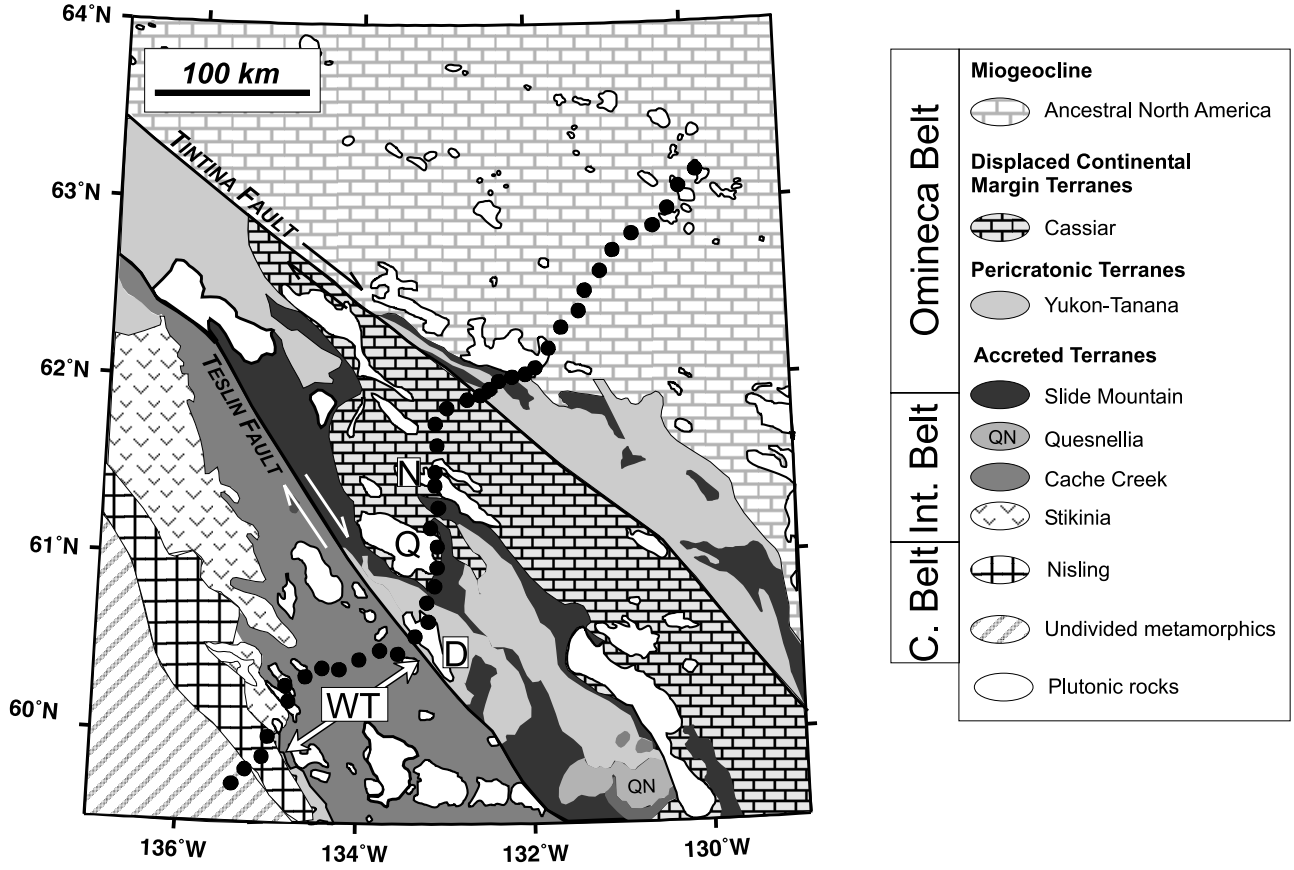

Figure 2. Terranes and tectonic elements map. The black dots represent the location of the magnetotelluric stations. N, Nitsulin batholith; Q, Quiet lake batholith; D, Deadman creek batholith; WT, Whitehorse trough.

eastward motion of the Farallon plate, and its subduction beneath the North American craton, occurred [*Irving and Wynne*, 1991]. This was followed by rapid and oblique convergence of the Kula plate relative to North America during latest Cretaceous and earliest Tertiary times and strike-slip deformation associated to the northwesterly motion of the Pacific plate relative to North America during the Tertiary [*Engebretson et al.*, 1984].

[6] The Canadian Cordillera can be divided into five major morphogeological and physiographic fault-bounded belts [*Gabrielse and Yorath*, 1991]. From west to east these belts are named the Insular Belt, the Coast Belt, the Intermontane Belt, the Omineca Belt, and the Foreland Belt, and their development reflects Mesozoic and Cenozoic collision and deformation along the northwestern margin of North America. The MT data presented here were acquired on the Coast, Intermontane, Omineca and Foreland Belts in southern Yukon and northwesternmost British Columbia.

[7] A recent study of Tertiary to recent alkaline lavas, many of which contain mantle xenoliths, across the northern Canadian Cordillera [*Abraham et al.*, 2001] shows that their chemical and isotopic characteristics can be correlated with their spatial position within the Coast, Intermontane, and Omineca Belts. There is a discontinuous change in the $^{87}Sr/^{86}Sr$ and $^{143}Nd/^{144}Nd$ ratios in recent alkaline basalts across the Tintina Fault. East of the fault, the erupted basalts have lower $^{87}Sr/^{86}Sr$ (0.7035) and higher $^{143}Nd/^{144}Nd$ (0.51295) ratios than equivalent basalts erupted west of the Tintina Fault, with $^{87}Sr/^{86}Sr$ >0.704 and $^{143}Nd/^{144}Nd$ in the range 0.51275–0.585. Important changes are also identified across both boundaries of the Intermontane Belt. Lavas erupted within the Intermontane Belt have lower $^{87}Sr/^{86}Sr$ (0.7028–0.7035) and higher $^{143}Nd/^{144}Nd$ (0.51292–0.513) concentrations compared with their equivalents in the Omineca Belt $^{87}Sr/^{86}Sr$ (>0.704), $^{143}Nd/^{144}Nd$ (0.51275–0.585) and Coast Belt $^{87}Sr/^{86}Sr$ (0.7035–0.7039), $^{143}Nd/^{144}Nd$ (0.5129). It is important to note that the boundary defined by the $^{87}Sr/^{86}Sr$ between the Coast Belt and the Intermontane Belt is located to the east of the surface boundary. The changes observed in the signatures of the alkaline basalts correspond approximately to isotopically distinctive upper crustal domains defined on the basis of granitoids in the northern Canadian Cordillera. However, the distinctive isotopic signatures of lavas erupted in each belt cannot be explained by crustal contamination, and are interpreted to be inherited from lithospheric mantle.

[8] The *P* wave velocity model for the upper mantle of the northern Canadian Cordillera of by *Frederiksen et al.* [1998], from teleseismic data (line BB′ on Figure 1), shows two significant velocity anomalies. *Frederiksen et al.* [1998] associate a high-velocity anomaly located beneath the Insular Belt with the edge of the subducting Pacific slab. The second feature is a large low-velocity anomaly elongated northwest-southeastward, and located beneath the

Intermontane Belt, that was interpreted to reflect a thermal anomaly with a possible compositional change. *Shi et al.* [1998] used the association of bimodal xenolith suites with this latter low *P* wave mantle velocity anomaly to suggest the presence of an anomalously hot (100–200°C hotter than surrounding lithosphere) asthenospheric mantle beneath the Insular Belt. This conclusion we address below.

[9] The average heat flow north of 59°N in the northern Canadian Cordillera is 105 mW/m^2, and temperatures calculated at Moho depths, using a conductive model, are high (800–1000°C) [*Lewis et al.*, 2002]. Active kinematics of the northern Canadian Cordillera are known from the Whitehorse-Yellowknife permanent GPS baseline and GPS velocities recently acquired by *Mazzotti and Hyndman* [2002]. GPS results indicate a northeast to north-northeast motion of the northern Canadian Cordillera, at about 5 mm/yr, relative to the stable North American Craton to the east. A kinematic and mechanical model of stress transfer developed by *Mazzotti and Hyndman* [2002] suggests a horizontal quasi-rigid displacement of the upper crust accommodated by a detachment in the weak lower crust.

[10] The seismic refraction/wide-angle reflection experiment carried out along Corridor 3 (B. Creaser and G. D. Spence, manuscript in preparation, 2004) indicates that the Tintina Fault is a crustal-scale feature across which significant structural differences occur. Another result from this study is the characterization of the upper crust of the Omineca Belt, west of the Tintina Fault, as a low-velocity anomaly centered at a depth of approximately 10 km. The seismic refraction data along Corridor 2 also shows a strong upper crustal expression across the Tintina Fault [*Welford et al.*, 2001].

[11] The most predominant pattern in the SNORCLE northern Canadian Cordillera seismic reflection experiment [*Cook et al.*, 2001] is the presence of a westward tapering lower crustal wedge of prominent reflectivity (WTW) that has been interpreted as Proterozoic sediments [*Snyder et al.*, 2002]. We note that in places, the WTW is defined by the onset of reflectivity, rather than by a subhorizontal reflector or package of reflectors. West of the TTF, within the WTW the reflectors are east dipping. Such a tapering wedge interpretation is similar to the one proposed by *Cook* [1995] for the southern Canadian Cordillera, although in the southern Canadian Cordillera data there was a prominent subhorizontal reflector marking the top of the wedge. The inferred crust-mantle transition is marked on seismic reflection sections by a sharp decrease in reflectivity along the entire length of Corridor 3 (at 11.5 s two-way travel time), although it is somewhat diffuse in the vicinity of the Tintina Fault and also shows a variation on the seismic reflection pattern below the Intermontane Belt. Another important result is the absence of strong laterally continuous crustal reflectors below the surface trace of the Tintina Fault.

3. Magnetotelluric Data and Regional Impedance Determination

[12] The magnetotelluric (MT) method involves measuring the temporal fluctuations of the horizontal components of the natural electromagnetic field on the surface to determine the lateral and vertical variations of electrical resistivity of the Earth's interior [*Vozoff*, 1991; *Jones*, 1992, and references therein]. Values of electrical resistivity of Earth materials in the crust and mantle are usually dominated by the presence of a minor constituent in the host rock matrix, and are thus complementary to bulk property physical parameters determined by seismic and potential field methods. The electrical resistivity of a rock depends not only on the amount of ionic and/or electronic conductors present but also on their interconnection and geometric distribution within the host rock [e.g., *ELEKTB Group*, 1997]. MT surveying is a useful technique for imaging tectonic and geodynamic processes that are difficult to sense remotely by other techniques [e.g., *Jones*, 1992]. When structures in the subsurface can be validly interpreted as having a significant strike extent, two-dimensional (2-D) modeling and inversion are appropriate. The MT responses for current flowing along structures is called the transverse electric (TE) mode, whereas the responses for current crossing structures is termed the transverse magnetic (TM) mode.

[13] The first step, prior to any geophysical interpretation of the MT responses, is to determine their dimensionality and directionality, and their variation with frequency, i.e., depth. To accomplish this, we have followed the steps outlined by *Groom et al.* [1993] on the basis of the *Groom and Bailey* [1989] method, using the multisite, multifrequency MT tensor decomposition code of *McNeice and Jones* [2001]. If the data are 2-D, this method facilitates estimation of the regional impedance tensor by detecting and removing most of the effects caused by local near-surface inhomogeneities. Figure 3 displays the geoelectric strike directions determined from the data at each site for the period range 0.01 – 5000 s in three period bands each two decades wide. The lengths of the strike arrows are scaled by the phase differences between the off-diagonal elements of the recovered regional 2-D impedance tensor (TM and TE modes); this gives a visual measure of sensitivity to strike direction. The gray shading of the square at each site indicates the normalized RMS (root mean square) misfit error between the observed and the estimated impedance; dark grey and black squares indicate averaged RMS misfits below 2. For all period bands the data can be considered 2-D with geoelectric strike direction close to −45°, which is parallel to the main geological features (Figure 1). The data from each site were fit to a frequency-independent 3-D/2-D distortion model, with an assumed strike angle of −45°, to determine the regional 2-D impedances. Most of the amplitude scaling effects, or static shifts [e.g., *Jones*, 1988], were removed during this process; the remaining site gain [*Groom and Bailey*, 1989], which is typically small, was accounted for as part of the inversion procedure.

4. A 2-D Inversion and Interpretation of Resistivity Model

[14] Joint 2-D inversions of the distortion-corrected TE and TM apparent resistivity and phase data were undertaken using the nonlinear conjugate gradients algorithm of *Rodi and Mackie* [2001]. The algorithm searches for the model that trades off the lowest possible misfit against the lowest possible roughness, measured by the sum of the lateral and vertical gradients in resistivity. The quality of the magnetic

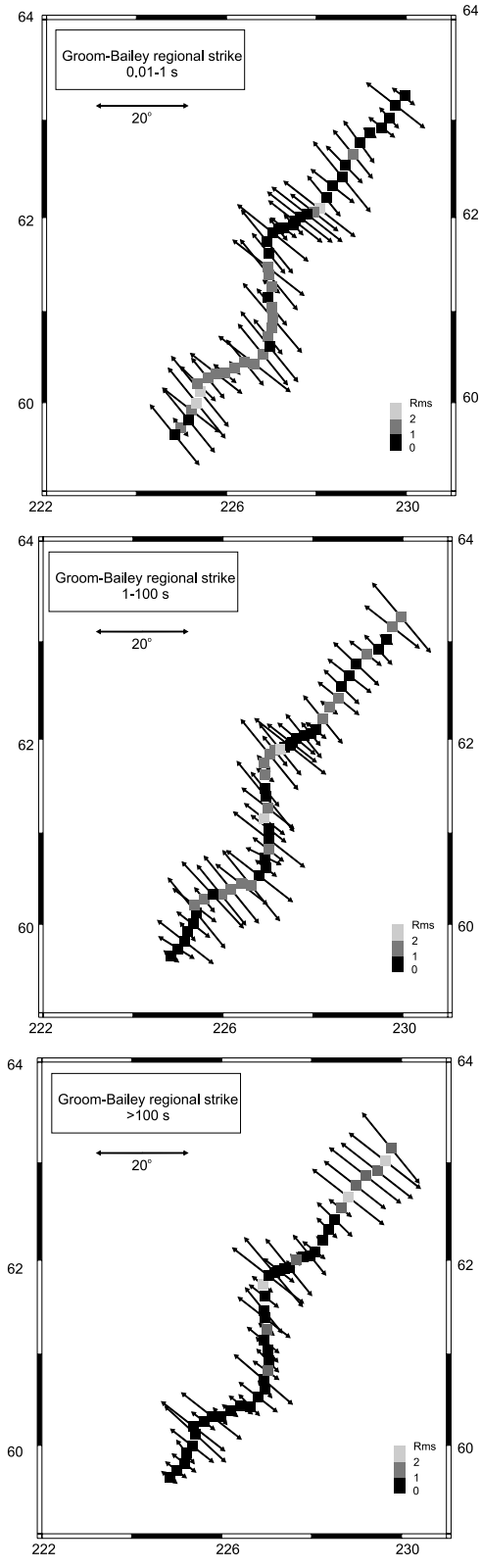

Figure 3. Regional azimuth determined using the *Groom and Bailey* [1989] distortion decomposition model for three different period bands between 0.01 and 5000 s. The length of the arrow is proportional to the average phase difference for the band.

transfer function data was rather poor, except at sites located close to the Tintina Fault [*Ledo et al.*, 2002b], and accordingly these data were not used during the inversion procedure. The final amplitude scalings of the apparent resistivities were determined as part of the inversion procedure. Neither structural features nor resistivity discontinuities were imposed during the inversion. The error floor adopted for the impedance tensor data was 5%; the model responses fit the apparent resistivity data to within 10%, and the phases to within 2.8°, on average. The final model derived is shown in Figure 4; comparisons between the data and model responses are shown in Figure 5 for the phases of both modes.

[15] The white lines on the model (Figure 4) correspond to the skin depth of an electromagnetic signal with a period of 5000 s (typically the longest period data at every other site), and the 10^{-4} isoline of the normalized weighted columnwise sums of the sensitivity matrix. The skin depth limit was calculated assuming that the electromagnetic signal in each block of the model has a 1-D behavior; this value must be interpreted as a conservative estimate of model depth resolution. The formal linear sensitivity matrix was calculated using the *Mackie et al.* [1997] 2-D inversion code following the ideas and the code modifications of *Schwalenberg et al.* [2002] and *Brasse et al.* [2002]. Figure 6 shows the TM, TE and joint TM + TE modes linear sensitivities for our model, calculated in terms of the logarithm of the apparent resistivities and phases. It is important to note that the values obtained represent the sensitivity (or influence on the data) to small perturbation of the logarithm of resistivity in each model cell. The near-surface structures are well defined by both modes. In contrast, the deeper structures seem to be controlled primarily by the TM mode data, except the most conductive part of the NE dipping conductive slab (see below). *Schwalenberg et al.* [2002] suggest choosing a minimum value of the sensitivity matrix to rule out the structures located outside this minimum, although the choice of this limit is an open question. We have chosen the same value as *Brasse et al.* [2002] in their MT study of the central Andes, namely, 10^{-4}; this value gives the same limit of resolution for the northeastern part of the model as the more simplistic 1-D skin depth calculation.

[16] From southwest to northeast the first-order regional lithospheric scale results from this MT model are as follows (numeric labels in Figure 4 correspond to the points below):

[17] 1. The presence of a NE dipping low-resistivity slab, starting in the middle-lower crust of the Coastal Belt that penetrates into the mantle below the Intermontane Belt. The crustal part of this slab has resistivity of 3–30 Ω m, whereas the mantle part has resistivity of 300–1000 Ω m.

[18] 2. A high resistivity lower crust and upper mantle below the Intermontane Belt.

[19] 3. A NE dipping region of low resistivity (~1000 Ω m) projects up to the surface to the defined boundary between the Intermontane and Omineca Belts, the Teslin Fault. The resistivity anomaly penetrates the whole crust, and possibly connects to a region of reduced resistivity in the mantle beneath the Omineca Belt, although that part of the model is poorly resolved.

[20] 4. The upper crust of the Omineca Belt is characterized by the presence of several low-resistivity structures.

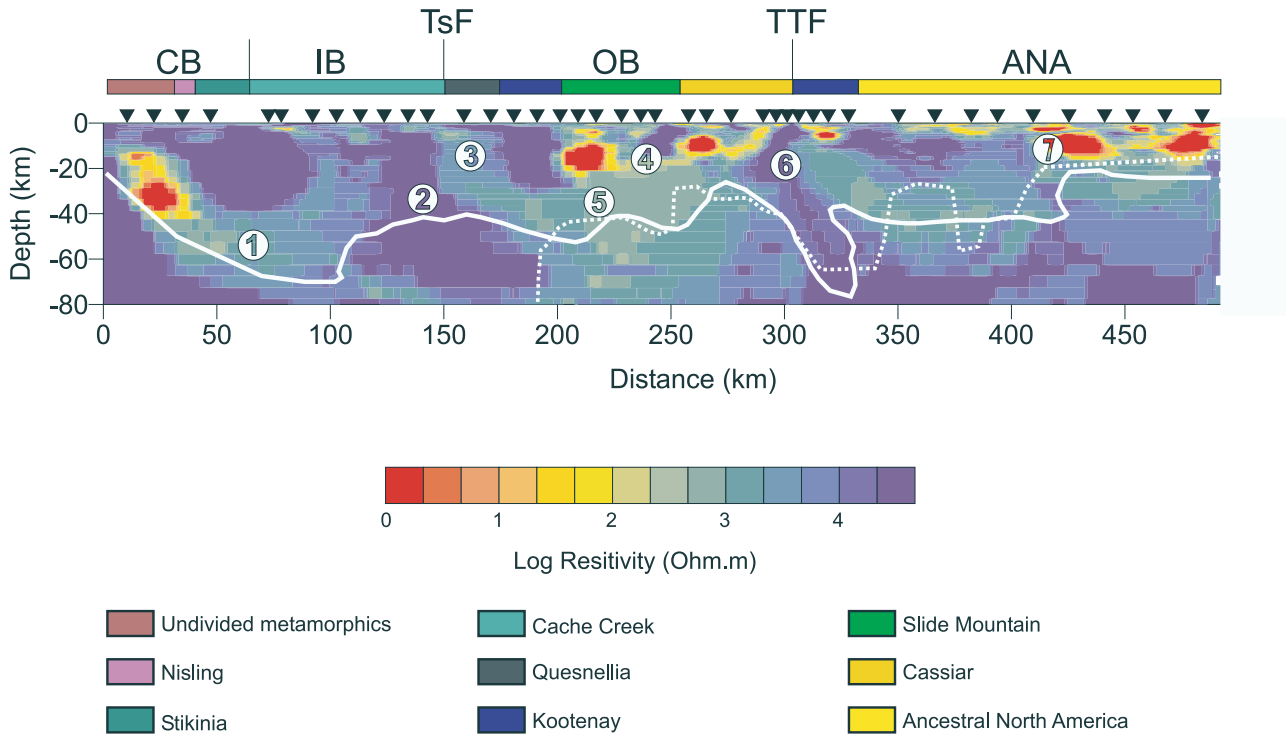

Figure 4. Two-dimensional MT resistivity model obtained by inversion using both TE and TM mode resistivities and phases. White solid line, isoline of 10^{-4} calculated from the linear sensitivity test; white dashed line, skin depth penetration for an electromagnetic signal with a period of 5000 s.

[21] 5. The Omineca Belt lower crust and upper mantle shows resistivity lower than the contiguous Intermontane Belt.

[22] 6. The Tintina Fault is imaged as a steep crustal-scale high resistivity subvertical feature that penetrates into the mantle with a NE dip.

[23] 7. The northeastern end of the model includes low-resistivity structures at upper crustal depths.

[24] The geological and tectonic implications of these structures, as well as comparison with other geophysical and geological data, are discussed below.

5. Discussion

5.1. Dipping Kula Plate: Feature 1

[25] The low resistivity values of the dipping conductive slab are constrained mainly by the TE mode data (Figure 6). This mode is usually more affected by 3-D effects (finite strike length, off-profile structures) than TM mode data [*Swift*, 1967; *Jones*, 1983; *Wannamaker et al.*, 1984], although the opposite has been shown to be true, for certain situations, by *Park and Mackie* [1997]. Such 3-D effects generally result in resistivity estimates that are too low. However, the tensor decomposition results for the longest periods at sites in the southeast of the profile show that the observed responses are consistent with a 2-D structure, or a 3-D structure that is sufficiently long that it can be considered 2-D. The observation of a similar dipping conductive structure in resistivity models for Corridor 2 to the south [*Wennberg*, 2003] suggests the structure has a significant along-strike length.

[26] The NE dipping low-resistivity slab below the Coast and Intermontane Belts lies above, and parallel to, a suite of reflectors located at mantle depths [*Cook et al.*, 2004]. These reflectors, labeled Ku in Figure 7, are interpreted by *Cook et al.* [2004] to be associated with convergent subduction of the Kula plate in the Paleocene [*Engebretson et al.*, 1984]. The isotopic characteristics of Eocene volcanic complexes lying north of the Yukon-British Columbia border, close to the western end of Corridor 3, suggest that their origin is also associated with plate subduction mechanisms [*Morris and Creaser*, 1998].

[27] The coincidence of the geometry of the conductor and the inferred position of the subducting slab provides a strong indication that the decreased resistivity is related to the Paleocene Kula plate subduction. Possible causes of the decreased resistivity include the presence of a small amount of an interconnected fluid phase, such as partial melt and/or free saline water trapped during the subduction, or the presence of a metallic conductor such as graphite, grain boundary carbon, or metallic oxides and sulphides occurring in metasedimentary rocks introduced into the crust during the subduction.

[28] The closest available heat flow measurement to the dipping conductor (from 100 km away) indicates a heat flow of 74 mW/m^2 (R. D. Hyndman, personal communication, 2000), which suggests, if anything, that the region closer to the coast is cooler than further inland. We take this result as excluding partial melt in the middle and lower crust as a possible explanation for the enhanced conductivity.

[29] Large conductors, comparable to the dipping conductor imaged in the present survey, have been identified elsewhere in the western part of the cordillera. MT studies across Vancouver Island [*Kurtz et al.*, 1986, 1990] and across the Cascade subduction zone in Washington and Oregon [*Wannamaker et al.*, 1989] also revealed the pres-

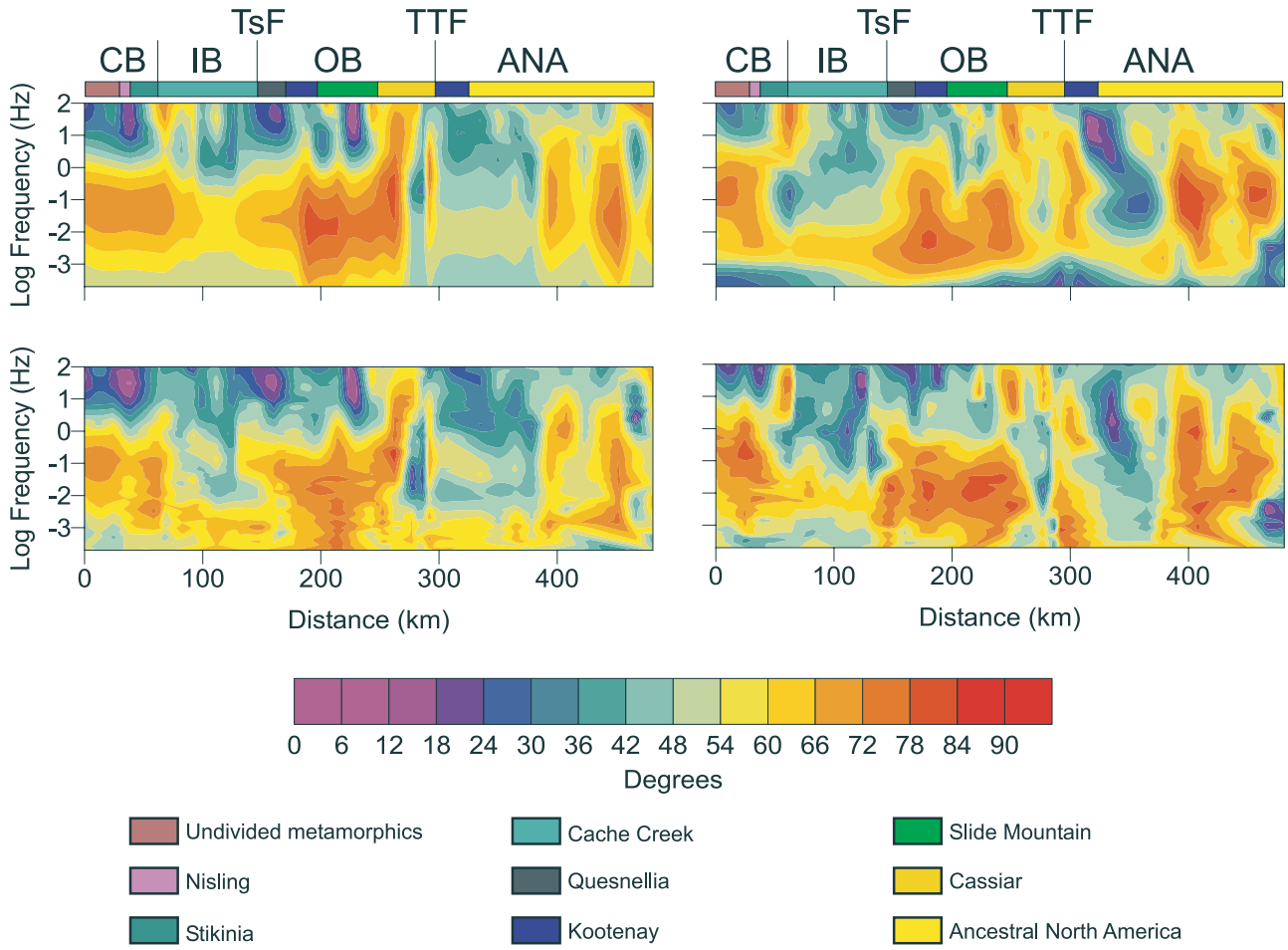

Figure 5. Comparison of phases from both TE and TM mode for (bottom) the data and (top) model responses. The final model fit the phase data within 2.8° in average that correspond to a 5% error floor of the impedance tensor data.

ence of a low-resistivity slab-like body. This layer was originally interpreted as being the subducting Juan de Fuca plate [*Kurtz et al.*, 1986; *Wannamaker et al.*, 1989] but subsequent work on the Vancouver Island transect demonstrated that these dipping conductive layers are not at the plate interface, but instead represent fluids that have risen buoyantly from the plate surface and are trapped beneath an impermeable isothermal barrier [*Jones*, 1987; *Hyndman*, 1988; *Cassidy and Ellis*, 1991, 1993].

[30] Several factors suggest that the dipping conductor on Corridor 3 is not caused by trapped fluids. It is particularly difficult to explain the dipping upper surface of the conductor with such an explanation. Active subduction in the area of the conductor ceased at around 50 Ma [*Engebretson et al.*, 1984] and, considering the crustal rheology and thermal conditions, it is unlikely that fluids would remained trapped for this duration. Isotopic studies of gold deposits in Alaska [*Goldfarb et al.*, 1991a, 1991b] suggest that crustal dewatering occurred on the transition to a transtensional regime in the crust. The models of the present stress accommodation in the northern Canadian Cordillera, determined by *Mazzotti and Hyndman* [2002], also suggest detachment in a weak lower crust, a situation inconsistent with long-term preservation of trapped fluids at these depths.

[31] *Stanley et al.* [1990] described a crustal conductor, adjacent to the Denali Fault system in the Alaska Range, which reaches a maximum depth of 20 km and has a subhorizontal form. *Stanley et al.* [1990] interpreted the observed anomaly as a consequence of underthrusting of carbonaceous flysch of the Gravina-Nutzotin sedimentary series during mid-Cretaceous convergence. *Mathez et al.* [1995], through the analysis of electrical conductivity measured in the laboratory from rock samples of this area, concluded that this midcrustal anomaly could be due to either underthrust flysch of the Gravina-Nutzotin sedimentary series, or intergranular graphite-bearing rocks of the overlying Yukon-Tanana terrane. To test these hypotheses, *Aleinikoff et al.* [2000] undertook an integrated Pb, Sr, Nd, and O isotopic study of Mesozoic and younger rocks that intruded the Yukon-Tanana terrane and Mesozoic Gravina-Nutzotin flysch units, in order to determine sources of the granitic rocks and to estimate the degree of involvement of the possible underlying flysch in silicic magma generation. Their results revealed a lack of a significant flysch-derived component in the Cretaceous and Tertiary granitic rocks of the Yukon-Tanana terrane, suggesting that the midcrustal anomaly may be caused by interconnected carbonaceous films in Yukon-Tanana terrane rocks, rather than flysch.

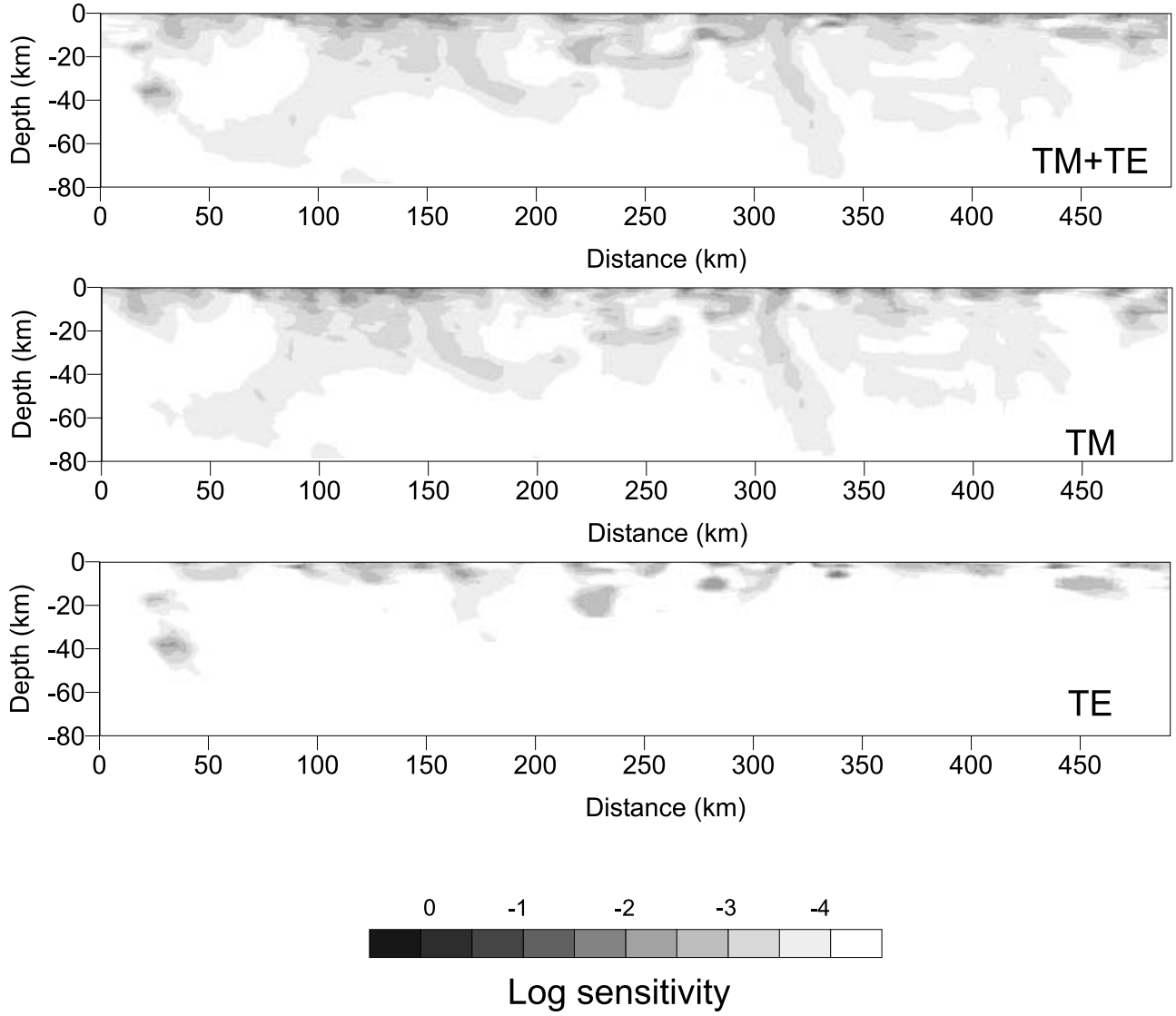

Figure 6. Contour of the normalized weighted columnwise sums of the sensitivity matrix. The graphics represent the influence on the data to small perturbations of the logarithm of resistivity in each model cell. (top) Sensitivity of TM and TE modes joint inversion; (middle) sensitivity of TM mode inversion; (bottom) sensitivity of TE mode inversion.

[32] The geological location of the conductor on Corridor 3 is similar to that of the conductor in Alaska, located 500 km to the northwest, although at different depths. Both conductors lie inboard of the Denali Fault and outboard of the extensive Stikinia terrane, and the conductor on Corridor 3 lies, in part, beneath rocks of the Nisling terrane (Figure 7), which is correlative with the Yukon-Tanana terrane [*Currie and Parish*, 1993]. Assuming a related source for the two conductors, the observed geometry of the conductor on Corridor 3 provides support for the *Stanley et al.* [1990] explanation of the Alaskan Range conductor. Considering the observed spatial correlation of the conductor on Corridor 3 with the path of the subducted Kula plate, it is unlikely that its source is in the overlying accreted terranes and it is more probable that its source is younger, metasedimentary rocks imbricated during subduction. The significant dip and mantle penetration of the Corridor 3 conductor both differ from the subhorizontal shape and upper crustal extent of the Alaska Range conductor. However, these differences are plausibly explained by the different angles of plate convergence at the two locations, and by the closer proximity of the Alaska Range conductor to the Denali Fault.

[33] The resistivity of the mantle part of the dipping conductor (300–1000 Ω m) is higher than in the crustal part (3–30 Ω m), and it is possible that the mechanism causing the decreased resistivity is different in the two regions. Processes by which subduction of oceanic crust can modify the resistivity structure of the mantle include: introduction of a component of conductive metasedimentary rocks; release of volatiles from the slab causing metasomatic alteration and partial melting of the overlying mantle rocks; and, in certain cases, through partial melting of the subducting slab. It is possible that the enhanced mantle conductivity is caused by the emplacement of carbonaceous and/or sulphidic metasedimentary rocks. It is argued above

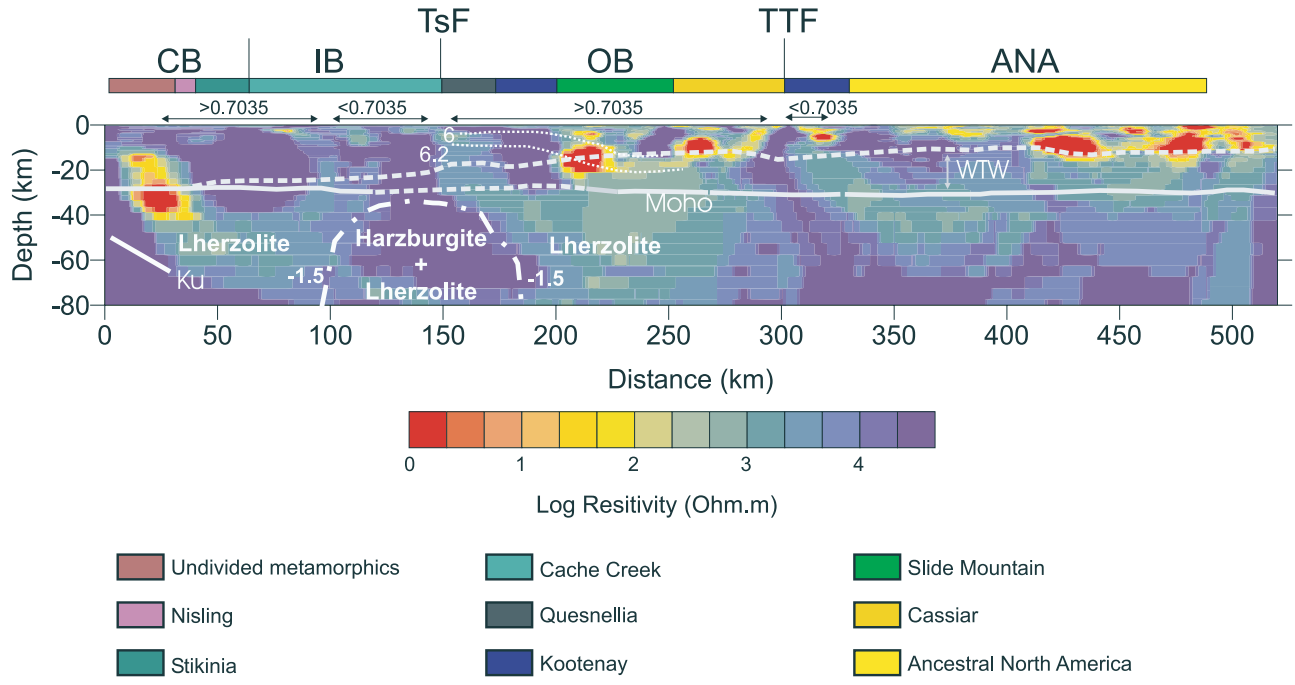

Figure 7. Comparison of the MT model with different geophysical and geological data. Dashed-dotted white line, *P* wave velocity (%) anomaly of *Frederiksen et al.* [1998]; gray line, westward tapering wedge, with the discontinuous sections in the Moho indicating the zones where there is a change in the seismic reflection pattern [*Cook et al.*, 2001]; white dotted line, velocity (km/s) determined from the seismic refraction experiment (B. Creaser and G. D. Spence, manuscript in preparation, 2004); $^{87}Sr/^{86}Sr$: Isotope data [*Abraham et al.*, 2001]. Ku, location of the seismic reflector associated to the Kula plate subduction.

that such rocks are associated with the subducting slab at crustal depths, so it is conceivable that a component of these rocks is also subducted into the mantle. It appears more likely that the enhanced mantle conductivity is caused by the introduction of H_2O-bearing fluids into the mantle wedge overlying the subducting slab. This process is consistent with the observed depth extent of the conductor, the upper surface of which extends to at least 70–80 km depth (Figure 7). As an oceanic slab penetrates the mantle, it can release fluids to depths of at least 125 km without melting, and a component of these volatiles may travel back up the slab some distance [*Eggler*, 1989]. The process is also consistent with the observed dipping nature of the conductor. One would expect the effects of the hydrous fluids to be greatest in the dipping region of the mantle overlying the subducting slab. In addition, it is possible that convection in the mantle wedge would reduce evidence of the hydration, except in a more stable dipping boundary layer above the descending slab [e.g., *Peacock*, 1996].

[34] Hydrous fluids could enhance mantle conductivity through several mechanisms. First, ionic conduction in a trapped fluid phase could cause a direct increase in conductivity. The elapsed time since the termination of subduction and the dipping upper surface of the conductor suggest this mechanism is unlikely occurring beneath Corridor 3. Second, the hydrous fluids could refertilize the lherzolitic to harzburgitic rocks in the overlying wedge to form phlogopite-bearing lherzolite. It has been suggested that phlogopite-rich rocks may have a low resistivity [*Boerner et al.*, 1999], but it is of note that the resistivity of such rocks has not been measured at the appropriate P-T conditions to confirm this condition in the mantle. More significantly, in xenoliths phlogopite usually is present in isolated crystals and never interconnected [*Jones et al.*, 2001]. Finally, the conductivity can be enhanced by the addition of small amounts of water to nominally anhydrous minerals [*Karato*, 1990]. This process provides a more effective method for increasing conductivity than does the presence of a small proportion of moderately conductive hydrous minerals such as phlogopite. It is also consistent with the observation of enhanced conductivity ~50 Ma after the cessation of subduction. We therefore favor this explanation for the observed enhanced mantle conductivity beneath the northwestern Coast Belt and southwestern Intermontane Belt.

5.2. Resistive Mantle Region Beneath the Eastern IB and Western Ob: Feature 2

[35] In Figure 4, the upper mantle structures below the Intermontane Belt are below the 10^{-4} limit of the linear sensitivity study. To test this further, we carried out a nonlinear sensitivity study of this part of the model, consisting of varying the resistivity values of the Intermontane upper mantle. The resistivity value was reduced from the 20,000 Ω m of the original model (Figure 4) to 300 Ω m, consistent with the resistivity of the upper mantle beneath the two bounding belts. Figure 8 shows the difference between the MT phases for both models. The TM mode data are most affected by the change on the upper mantle resistivity, increasing the phase values by up to 20° (decreasing the apparent resistivity), and in the TE mode the increase is up to 8°. To determine the lower limit of mantle resistivity

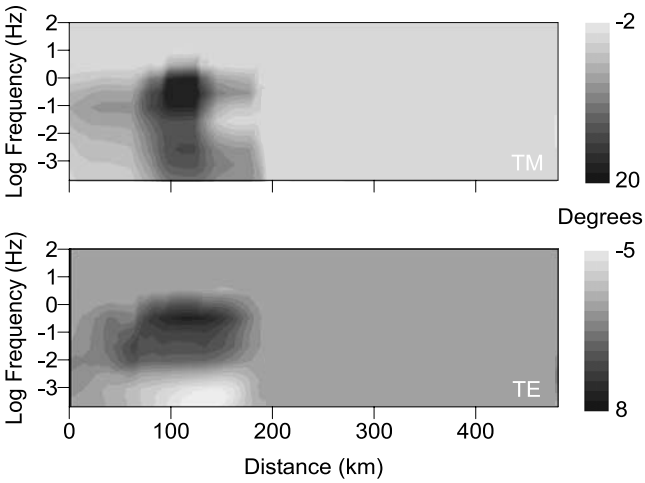

Figure 8. Comparison of phase difference between our final model (Figure 4) and an alternative model with an electrical resistivity of 300 Ω m for the mantle below the Intermontane Belt.

compatible with our model, the response of the model was calculated for progressively decreasing values of mantle resistivity, and Figure 9 shows the average maximum difference for the different models. The TM mode is more affected by decreasing of the resistivity of the mantle; the lower limit for the mantle resistivity in this region is 5000 Ω m.

[36] This sharp lateral step change of the mantle resistivity below the Intermontane Belt (Figure 7) correlates spatially with both a change in the seismic reflection pattern of the Moho discontinuity [*Snyder et al.*, 2002] and with geochemical data from the recent alkaline basalts of *Abraham et al.* [2001], suggesting at mantle depths an eastern displacement from the surface tectonic boundary between the Coast and Intermontane Belts. Moreover, the boundary limit coincides roughly with the western boundary of the low-velocity mantle anomaly of *Frederiksen et al.* [1998]. This low-velocity anomaly, taken together with the existence of bimodal xenoliths (lherzolites and harzburgites) in this area, was considered by *Shi et al.* [1998] as evidence of a region of elevated hot asthenospheric mantle due to the presence of a thermal plume linked with the Late Cretaceous Carmacks Group [*Johnston et al.*, 1996]. The maximum difference in equilibration temperatures calculated for the lherzolites and harzburgites is 60–80°C. The preferred explanation by *Frederiksen et al.* [1998] for their velocity anomaly is the presence of asthenospheric material upflow driven by the opening of a slab window beneath the northern Cordillera [*Thorkelson and Taylor*, 1989; *Thorkelson*, 1996]; the velocity anomaly is explained by a 100–200°C mantle temperature increase.

[37] The expected resistivity of the anomalous mantle region can be determined using the mineral composition of the xenoliths [*Shi et al.*, 1998] and their resistivity values determined in laboratory experiments [*Constable et al.*, 1992; *Xu and Shankland*, 1999; *Xu et al.*, 2000]. The lherzolite xenoliths contain 15% clinopyroxene (Cpx), 25% orthopyroxene (Opx) and 60% olivine on average, whereas the harzburgite xenoliths contain 2% Cpx, 18% Opx, and 80% olivine on average. *Shi et al.* [1998] concluded that the harzburgites xenoliths represent the partial melt residue of lherzolite lithospheric mantle. The resistivity values for these minerals in the temperature range between 1000 and 1200°C are as follows: Cpx (14,200–1400 Ω m), Opx (2500–200 Ω m), and olivine (5200–700 Ω m) (calculated from parameters listed by *Xu et al.* [2000]). It is clear from these values and the mineral percentage determined for the xenoliths that independently of the mixing law employed to calculate the effective resistivity, temperature must be closer to 1000°C rather than 1200°C. Thus our MT model supports a small increase in mantle temperature below the Intermontane Belt more in accordance with the equilibration temperatures calculated for the lherzolites and harzburgites, but not an increase of the order of 200°C suggested by *Frederiksen et al.* [1998].

[38] Finally, there is an apparent eastern displacement at mantle depths of the geoelectric and isotopic signature between the Intermontane and Coast Belts from the tectonic boundary at the surface. This suggests that lherzolitic lithosphere extends partly beneath the Intermontane Belt.

5.3. Resistive Lower Crust in Eastern CB and IB: Feature 2

[39] Another major feature of the model is the high resistivity lower crust below the eastern part of the Coast Belt and the Intermontane Belt. This is in stark contrast to the pervasive nature of the reduced lower crustal resistivity of the southern part of the Southern Canadian Cordillera [*Ledo and Jones*, 2001], interpreted to be due to interconnected aqueous fluids. The values observed in the northern Canadian Cordillera are in agreement with the values observed in the central and northern parts of the southern Canadian Cordillera [*Ledo and Jones*, 2001]. The along-strike differences observed in the southern Canadian Cordillera were associated with the short-lived Eocene extension experienced by the southern part of the Omineca Belt [*Parrish et al.*, 1988]. Along Corridor 3, the values of resistivity observed can be explained by hot, dry lower crustal rocks [*Olhoeft*, 1981; *Shankland and Ander*, 1983].

5.4. Teslin Fault: Feature 3

[40] The Teslin Fault (Figure 2) represents the boundary between the Intermontane and Omineca Belts. In this region

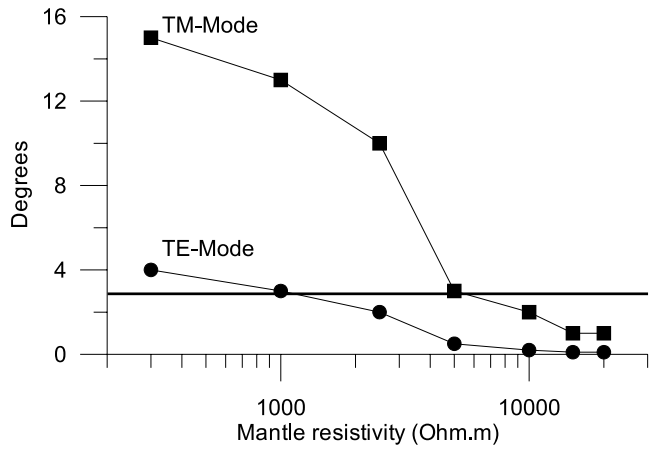

Figure 9. Average maximum misfit for different Intermontane Belt mantle resistivities.

the Omineca Belt is represented by the boundary between a major accreted terrane, Stikinia, and displaced continental margin rocks of the Cassiar terrane. The interpreted role and significance of the Teslin structural zone in the tectonic evolution of the northern Canadian Cordillera has changed significantly over the last decade. It was first described as a westerly dipping subduction zone by *Tempelman-Kluit* [1979]. This subduction model was widely accepted with slight adjustments [*Erdmer*, 1985; *Hansen*, 1986] to include strike-slip faulting and other events. *Brown et al.* [1995], and later *Stevens and Erdmer* [1996], questioned this subduction interpretation. Currently, there is a vigorously debated controversy about the presence of a lithospheric-scale suture based on different interpretation of geological data [*Hansen and Dusel-Bacon*, 1998; *de Keijzer et al.* 1999, 2001; *Oliver et al.*, 2001]. In the model proposed recently by *de Keijzer et al.* [1999, 2001], the Teslin zone is a young structure resulting from post-accretionary folding, instead of a fundamental lithospheric boundary [*Hansen and Dusel-Bacon*, 1998; *Oliver et al.*, 2001].

[41] In our model the Teslin Fault is characterized by a steep, listric, northeast dipping zone, of medium to low resistivity (~1000 Ω m), which penetrates the whole crust. This structure correlates well with the east dipping reflectors observed in the seismic reflection section [*Snyder and Roberts*, 2001]. At middle and lower crustal depths, the electrical resistivity model indicates a near-vertical boundary below the Teslin Fault, separating rocks of higher resistivity in the southwest from more conductive rocks beneath the Omineca Belt. This abrupt change can be observed particularly in the phase data (Figure 5). Our result contrasts sharply with the interpretation of the seismic reflection data by *Cook et al.* [2001], *Erdmer et al.* [2001] and *Snyder et al.* [2002], who suggested the existence of a continuous westward thinning reflective layered zone in the middle and lower crust (WTW in Figure 7).

5.5. Omineca Belt Upper Crust: Feature 4

[42] Between the Teslin and Tintina Faults lies the northern Omineca Belt, a collage of complex geological structures formed as a result of rifting, subduction, arc-continent collision and obduction since the Early Mississippian (350 Ma) [*Tempelman-Kluit*, 1979]. The upper crust of the Omineca Belt includes several low-resistivity structures that correlate spatially with a low-velocity zone determined by seismic refraction data (B. Creaser and G. D. Spence, manuscript in preparation, 2004). It is speculated that the low-resistivity structures observed below the Cassiar terrane are associated with metamorphosed graphite-bearing sediments. Similar low-resistivity structures are also present in the preliminary interpretation of MT data along Corridor 2 [*Wennberg et al.*, 2002], suggesting the source of the decreased resistivity must occur over a reasonably large spatial scale. Rocks exposed on Cassiar terrane surface contains graptolite shale [*Monger*, 1989] indicating the presence of carbonaceous rocks. Also, in order to produce such low resistivities with fluids would require large volumes of saline fluids that, at this depth (20 km), would be gravitationally unstable. The more resistive regions present in the upper crust between the conductors could be associated with intrusive rocks; Middle Cretaceous plutonism in this area produced the Nitsulin, Quiet Lake and Deadman Creek batholiths [*Tempelman-Kluit*, 1979] (Figure 2).

Table 1. Average Maximum Misfit for Different Omineca Belt Mantle Resistivities

Omineca Belt Upper Mantle Resistivity, Ω m	Average Maximum Misfit, deg	
	TE Mode	TM Mode
1,000	0.5	1.7
2,500	1.4	4.5
6,300	1.8	9.0
15,000	2.0	12.0

5.6. Omineca Belt Lower Crust: Feature 5

[43] The Omineca Belt lower crust is characterized by values between 500 and 1000 Ω m on both sides of the Tintina Fault. These values are comparable to the ones obtained by *Ledo and Jones* [2001] in the northernmost MT models of the southern Canadian Cordillera, and would imply the absence of significant amounts of interconnected free fluids. For the upper mantle we carried out a nonlinear sensitivity analysis similar to the one undertaken for the Intermontane Belt upper mantle. Resistivity of the feature was increased from the original model (Figure 4) to 15,000 Ω m, consistent with the resistivity of the upper mantle beneath the Intermontane Belt. Again, the TM mode data are most affected by the change on the upper mantle resistivity (Table 1). The upper limit of the Omineca upper mantle resistivity is 1000 Ω m. The low resistivity in the Omineca mantle correlates with the low-velocity, low-density mantle noted by *Welford et al.* [2001] in Corridor 2.

5.7. Tintina Fault: Feature 6

[44] The Tintina Fault is imaged as a subvertical, crustal-scale, high-resistivity feature throughout its whole crustal extent. The electrical resistivity structure of the fault shows similar characteristics along the three MT profiles crossing it, and its possible geological interpretations were discussed by *Ledo et al.* [2002b]. The absence of a conducting zone at mid to lower crustal levels below the surface trace of the Tintina Fault may be attributed to the absence of circulating meteoritic or metamorphic fluids at this depth, or to the physical conditions within the fault that did not permit the precipitation of graphite from CO_2-rich fluids. The change in Sr and Nd isotopic ratios across the Tintina Fault, $^{87}Sr/^{86}Sr > 0.704$ to the west and $^{87}Sr/^{86}Sr = 0.7035$ to the east [*Abraham et al.*, 2001], indicates that it separates two lithospheric mantles with different origins. Comparison of the seismic reflection data [*Cook et al.*, 2001] and the resistivity model for Corridor 3 shows a good correlation between the high-resistivity zone and the absence of reflectors. The coincidence of fault zones transparent to both seismic and electrical methods implies that the fault could be considered healed [*Eberhart-Phillips et al.*, 1995]. This result agrees with the present-day low seismic activity at the Tintina Fault [*Lowe et al.*, 1994].

5.8. Upper Crust of Ancestral North America: Feature 7

[45] To the northeast of the Tintina Fault, the geological structure consists of thick sequences of early to mid-Proterozoic carbonate and siliclastic rocks deposited along

the Proterozoic rifted margin of North America, overlain by a passive margin miogeoclinal sequence containing rocks ranging in age from Proterozoic to Devonian [*Gabrielse and Yorath*, 1991]. During the Jurassic to Paleocene Cordilleran deformation the passive margin sequences were folded and thrust onto the edge of Ancestral North America, forming the Foreland Belt. In the northeast part of Corridor 3 the basement rocks consist of rocks of the MacKenzie Mountain Supergroup and the overlying Windermere Supergroup [*Snyder et al.*, 2002]. The surface rocks are part of the Selwyn Basin, which contains Precambrian to Middle Devonian deeper water offshore deposits [*Gordey and Anderson*, 1993]. The sedimentary rocks include a thick sequence of black carbonaceous shales. Several important SEDEX deposits are located near McMillan Pass at the northeast end of the corridor [*Gordey and Anderson*, 1993].

[46] The shallow (upper 5 km) conductors near the northeast end of Corridor 3 occur within the rocks of the Selwyn Basin. It is possible that the conductors may be associated with individual mineral deposits. Given the spatial distribution of the MT sites and the smoothing characteristics of the inversion code used, the size of the low-resistivity upper crustal structures is possibly overestimated, and their resistivities overestimated. However, it is more probable that the conductors are associated with more widespread rocks of the Selwyn basin. The carbonaceous shales represent the most probable source. The temperatures associated with the regional metamorphic grade of subgreenschist facies [*Gordey and Anderson*, 1993] are lower than the 400° required to cause graphitization at low pressure, but it has been speculated that graphitization can occur in relatively low temperatures in appropriate geological strain regimes [*Boerner et al.*, 1996].

[47] An alternative explanation is required for the conductors at the northeast end of Corridor 3 located at depths of around 10 km. These conductors (resistivity <10 Ω m) are located within rocks interpreted to form part of the Proterozoic Windermere and MacKenzie Mountain supergroups [*Snyder et al.*, 2002]. The enhanced conductivity may be explained by the presence of conductive rock units within these sequences. However, the WTW is also interpreted to consist of rocks of the Windermere and Mackenize Mountain Supergroups along with the underlying Proterozoic sequences (the Muskaw Assemblage and Wernecke Supergroup) and, within the survey area, the wedge does not contain any zones of comparable low resistivity. It is of note that the deeper conductors in both the Omineca Belt and the northeast of the corridor lie near the interpreted upper margin of the WTW (Figure 7). It is possible that both sets of conductors have a similar origin, and are associated with the deformation that occurred during the thrusting of younger rocks over the Proterozoic crustal wedge.

5.9. Tectonic Implications

[48] Magnetotelluric studies in the southern Canadian Cordillera revealed a resistive upper crust and reduced resistivity in the lower crust, which cannot, in general, be associated with a particular geological terrane [*Jones and Gough*, 1995; *Ledo and Jones*, 2001]. There is though some spatial association of lower crustal resistivity with larger-scale major fault-bounded belts [*Jones et al.*, 1988]. In contrast, the structure of the northern Canadian Cordillera is far more complex, and exhibits significant changes in the whole crust between different terranes within the same belt. Such variability can also be observed in the upper crustal velocities within the Omineca Belt (B. Creaser and G. D. Spence, manuscript in preparation, 2004) (see Figure 7). It is also important to note the lack of correlation between the westward tapering wedge (WTW), interpreted from the seismic reflection data, and the electrical resistivity distribution. There are two likely end-members to explain this: (1) The electrical resistivity variations within the WTW, associated with North America lower crust, are inherent to the origin of the Proterozoic sediments or (2) these variations were caused during the different accretionary episodes. Given the regional scale of the WTW, it is possible that some differences in its electrical properties are inherent to it. During the accretionary history it is likely that both redistribution of conductive material, due to stress fields and migration of fluids/partial melting from the lithosphere of subducted terranes through the WTW, would affect the electrical resistivity. However, there is a significant difference compared to the southern Canadian Cordillera, where postaccretionary processes homogenized the electrical resistivity of the lower crust, while in the northern Canadian Cordillera these processes, if they occurred, were more localized and less important. Another important difference between the electrical resistivity models obtained in the southern Canadian Cordillera and the model obtained here, is that the lack of high lower crustal conductivity allows us to characterize the resistivity of the upper mantle.

[49] The difference observed across the northern Canadian Cordillera mantle lithosphere beneath the different belts could be developed by tectonic imbrication during the subduction of the lithosphere of the accreted terranes. This hypothesis has important consequences, because it implies that the ancestral North America mantle root was removed, or deeply underthrusted, during different subduction episodes. Moreover, this interpretation agrees with the geochemical study of alkaline volcanic centers of *Abraham et al.* [2001] where lithospheric domains with distinct isotopic signatures were characterized. A similar mechanism, based on the tectonic imbrication of one or more slabs subducted, has been proposed to explain the Archean lithospheric tectonic evolution in the Kapvaal Craton [*Helmstaedt and Schulze*, 1989] and in the Slave Craton [*Davis et al.*, 2003]. This hypothesis would favor relatively shallow or low angle subduction during the different accretionary processes. This idea has already been proposed by *Monger et al.* [1985] and *Page et al.* [1986] for the Western Cordillera of North America based on deep seismic reflection profiling undertaken in Alaska. If the dipping crust-mantle conductor observed beneath the Coast Belt is indeed mapping the path of the subducting slab then it may imply a change in the dip of the subduction with distance inland.

6. Conclusions

[50] The MT data acquired along Lithoprobe SNORCLE Corridor 3 in northern British Columbia and southern Yukon has been modeled with a 2-D electrical resistivity model with a strike of −45°, parallel to the main tectonic

features. The model, obtained from distortion-corrected regional data, reveals several structures that constrain possible tectonic evolution models of the northern Canadian Cordillera. Below the Coast Belt, the presence of a northeast dipping low-resistivity slab in the lower crust has been associated with the Paleocene subduction of the Kula plate. The low resistivity values observed in the crust cannot be explained by the presence of fluids and/or partial melt given the rheology and thermal conditions of this zone described by other authors. Comparison of our results with MT studies in the Alaskan Range [*Stanley et al.*, 1990] and assuming a related source for the observed anomalies supports an interpretation in terms of metasedimentary rocks imbricated during subduction. On the other hand, the enhanced conductivity at mantle depths is more likely due to the introduction of H_2O-bearing fluids. This conductive structure represents the geoelectrical boundary between the Coastal and Intermontane Belts at mantle depths. A significant result is that this boundary is displaced to the northeast, with respect to the surface boundary, and coincides with the Coast and Intermontane Belt mantle transition determined by geochemistry and isotopic data [*Abraham et al.*, 2001].

[51] The geoelectrical model allows an interpretation of the inheritance of the crust beneath the accreted terranes. For example, in the upper crust of the Omineca Belt, beneath the accreted terranes high resistivity structures are interpreted in terms of the presence of batholiths of middle Cretaceous age. Low-resistivity structures found in the upper crust may be due to the presence of metamorphosed sediments. The lower crust of the Omineca Belt can be interpreted as having an absence of fluids, in a similar manner as the central Omineca Belt of the southern Canadian Cordillera [*Ledo and Jones*, 2001].

[52] The MT model provides new information about the depth extent and geometry of the main fault systems, namely the Teslin suture zone and the Tintina Fault. The electrical image of the Teslin suture zone is characterized by a listric zone of medium electrical resistivity that penetrates the whole crust. The Tintina Fault also penetrates the whole crust, and it is transparent to electric and seismic methods. As a final point, it is important to note the strong lateral variation at depth observed in the geoelectrical model, indicating the complex structural evolution of the lithospheric mantle during the superimposed episodes of subduction, seafloor spreading and transform faulting.

[53] **Acknowledgments.** The financial support for this project came from Lithoprobe and the Geological Survey of Canada. Geosystem Canada collected the broadband data. Jessica Spratt and Grant Wennberg acquired the long-period data. D. Snyder and J. Craven provided helpful comments on this work. We thank C. Roots, D. Murphy, and all the people of the Yukon Geology Program for their assistance. We thank Lincoln Hollister, Phil Wannamaker, and the Associate Editor for their substantial comments on our original version of this manuscript. J.L. thanks Lithoprobe and the Geological Survey of Canada for supporting his Visiting Fellowship in Ottawa. Geological Survey of Canada contribution 2003002.

References

Abraham, A. C., D. Francis, and M. Polvé (2001), Recent alkaline basalts as probes of the lithospheric mantle roots of the northern Canadian Cordillera, *Chem. Geol.*, *175*, 361–386.

Aeinikoff, J. N., Farmer, G. L. R. O. Rye, and W. J. Nokleberg (2000), Isotopic evidence for the sources of Cretaceous and tertiary granitic rocks, east-central Alaska: Implications for the tectonic evolution of the Yukon-Tanana terrane, *Can. J. Earth Sci.*, *37*, 945–956.

Boerner, D., R. D. Kurtz, and J. A. Craven (1996), Electrical conductivity and Paleo-Proterozoic foredeeps, *J. Geophys. Res.*, *101*, 13,775–13,791.

Boerner, D. E., R. D. Kurtz, J. A. Craven, G. M. Ross, F. W. Jones, and W. J. Davis (1999), Electrical conductivity in the Precambrian lithosphere of western Canada, *Science*, *283*, 668–670.

Brasse, H., P. Lezaeta, V. Rath, K. Schwalenberg, W. Soyer, and V. Haak (2002), The Bolivian Altiplano conductivity anomaly, *J. Geophys. Res.*, *107*(B5), 2096, doi:10.1029/2001JB000391.

Brown, R. L., S. D. Carr, J. L. Harvey, P. F. Williams, and M. de Keizer (1995), Structure and tectonic significance of the Teslin suture zone, Lithoprobe; Slave-Northern Cordillera Lithospheric Evolution (SNORCLE); report of 1995 transect meeting, *Lithoprobe Rep. 44*, pp. 56–62, Univ. of B. C., Lithoprobe Secr. for the Can. Lithoprobe Program, Vancouver.

Cassidy, J. F., and R. M. Ellis (1991), Shear wave constraints on a deep crustal reflective zone beneath Vancouver Island, *J. Geophys. Res.*, *96*, 19,843–19,851.

Cassidy, J. F., and R. M. Ellis (1993), *S* wave velocity structure of the northern Cascadia subduction zone, *J. Geophys. Res.*, *98*, 4407–4421.

Clowes, R. M., F. A. Cook, A. G. Green, C. E. Keen, J. N. Ludden, J. A. Percival, G. M. Quinlan, and G. F. West (1992), Lithoprobe: New perspective on crustal evolution, *Can. J. Earth Sci.*, *29*, 1813–1864.

Clowes, R. M., F. A. Cook, and J. N. Ludden (1998), Lithoprobe leads to new perspectives on continental evolution, *GSA Today*, *8*, 1–7.

Constable, S., T. J. Shankland, and A. Duba (1992), The electrical conductivity of an isotropic olivine mantle, *J. Geophys. Res.*, *97*, 3397–3404.

Cook, F. A. (1995), The reflection Moho beneath the southern Canadian Cordillera, *Can. J. Earth Sci.*, *32*, 1520–1530.

Cook, F. A., R. M. Clowes, D. B. Snyder, A. J. van der Verden, K. W. Hall, P. Erdmer, and C. Evenchick (2001), Lithoprobe seismic reflection profiling of the northern Canadian Cordillera: First results of the SNORCLE profiles 2 and 3, in *SNORCLE Trancset and Cordilleran Tectonics Workshop Meeting*, compiled by F. Cook and P. Erdmer, *Lithoprobe Rep. 79*, pp. 36–49, Univ. of B. C., Lithoprobe Secr. for the Can. Lithoprobe Program, Vancouver.

Cook, F. A., R. M. Clowes, D. B. Snyder, A. J. van der Velden, K. W. Hall, P. Erdmer, and C. A. Evenchick (2004), Precambrian crust and lithosphere beneath the northern Canadian Cordillera discovered by Lithoprobe seismic reflection profiling, *Tectonics*, *23*, doi:10.1029/2002TC001412, in press.

Currie, L., and R. R. Parish (1993), Jurassic accretion of Nisling terrane along the western margin of Stikinia, Coast Mountains, northwestern British Columbia, *Geology*, *21*, 235–238.

Davis, W., A. G. Jones, W. Bleeker, and H. Grutter (2003), Lithospheric development in the Slave Craton: Linked crustal and mantle perspective, *Lithos.*, *71*, 575–589.

de Keijzer, M., P. F. Williams, and R. L. Brown (1999), Kilometre-scale folding in the Teslin Zone, northern Canadian Cordillera, and its tectonic implications for the accretion of the Yukon-Tanana Terrane to North America, *Can. J. Earth Sci.*, *36*, 479–494.

de Keijzer, M., M. G. Mihalynuk, and S. T. Johnston (2000), Structural investigation of an exposure of the Teslin Fault, northwestern British Columbia, in *Current Research*, 10 pp., Geol. Surv. of Can., Ottawa.

de Keijzer, M., P. F. Williams, and R. L. Brown (2001), Kilometre-scale folding in the Teslin Zone, northern Canadian Cordillera, and its tectonic implications for the accretion of the Yukon-Tanana Terrane to North America, discussion and reply, *Can. J. Earth Sci.*, *38*, 879–887.

Eberhart-Phillips, D., W. D. Stanley, B. D. Rodriguez, and W. J. Lutter (1995), Surface seismic and electrical methods to detect fluids related to faulting, *J. Geophys. Res.*, *100*, 12,919–12,936.

Eggler, D. H. (1989), Influence of H_2O and CO_2 on melt and fluid chemistry in subduction zones, in *Crust/Mantle Recycling at Convergence Zones*, *NATO ASI Ser. C*, vol. 258, edited by S. R. Hart and L. Gülen, Kluwer, pp. 97–104, Kluwer Acad., Norwell, Mass.

ELEKTB Group (1997), KTB and the electrical conductivity of the crust, *J. Geophys. Res.*, *102*, 18,289–18,305.

Engebretson, D. C., A. Cox, and R. G. Gordon (1984), Relative motions between oceanic plates of the pacific basin, *J. Geophys. Res.*, *89*, 10,291–10,310.

Erdmer, P. (1992), Ecoglitic rocks in the St. Cyr klippe, Yukon, and their tectonic significance, *Can. J. Earth Sci.*, *29*, 1296–1304.

Erdmer, P. (1985), An examination of the cataclastic fabrics and structures of parts of Nisutlin, Anvil and Simpson allochthons, central Yukon: Test of the arc-continent collision model, *J. Struct. Geol.*, *7*(1), 57–72.

Erdmer, P., F. Cook, R. Clowes, D. Snyder, C. Evenchik, A. van der Velden, and K. Hall (2001), Some geological constraints on Cordilleran structure

imposed by line 3 reflections—MacMillan Pass to White Pass, in *SNORCLE Trancset and Cordilleran Tectonics Workshop Meeting*, compiled by F. Cook and P. Erdmer, *Lithoprobe Rep.* 79, pp. 54–55, Univ. of B. C., Lithoprobe Secr. for the Can. Lithoprobe Program, Vancouver.

Frederiksen, A. W., M. G. Bostock, J. C. VanDecar, and J. F. Cassidy (1998), Seismic structure of the. upper mantle beneath the northern Canadian Cordillera from teleseismic travel-time inversion, *Tectonophysics*, *294*, 43–55.

Gabrielse, H., and C. J. Yorath (1991), Introduction, in *The Geology of North America*, vol. G-2, *Geology of the Cordilleran Orogen in Canada*, edited by H. Gabrielse and C. J. Yorath, pp. 15–59, Geol. Soc. of Am., Boulder, Colo.

Goldfarb, R. J., L. W. Snee, L. D. Miller, and R. J. Newberry (1991a), Rapid dewatering of the crust deduced from ages of mesothermal gold deposits, *Nature*, *354*, 296–298.

Goldfarb, R. J., R. J. Newberry, W. J. Pickthorn, and C. A. Gent (1991b), Oxygen, hydrogen, and sulfur isotope studies in the Juneau Gold Belt, southeastern Alaska: Constraints on the origin of hydrothermal fluids, *Econ. Geol.*, *86*, 66–80.

Gordey, S. P., and R. G. Anderson (1993), Evolution of the northern Cordilleran Miogeocline, Nahanni map area [105I], Yukon and Northwest Territories, *Mem. Geol. Surv.*, 428.

Groom, R. W., and R. C. Bailey (1989), Decomposition of magnetotelluric impedance tensors in the presence of local three-dimensional galvanic distortion, *J. Geophys. Res.*, *94*, 1913–1925.

Groom, R. W., R. D. Kurtz, A. G. Jones, and D. E. Boerner (1993), A quantitative methodology for determining the dimensionality of conductivity structure and the extraction of regional impedance responses from magnetotelluric data, *Geophys. J. Int.*, *115*, 1095–1118.

Hansen, H. L. (1986), Petrotectonic study of the Teslin suture zone, Yukon: A progress report, *Yukon Geol. 1*, pp. 125–130, Indian and North. Affairs Can., Whitehorse, Yukon Territory.

Hansen, V. L., and C. Dusel-Bacon (1998), Structural and kinematic evolution of the Yukon-Tanana upland tectonites, east-central Alaska: A record of late Paleozoic to Mesozoic crustal assembly, *Geol. Soc. Am. Bull.*, *110*(2), 211–230.

Helmstaedt, H. H., and D. J. Schulze (1989), Southern African kimberlites and their mantle sample: Implications for Archean tectonics and lithosphere evolution, in *Kimberlites and Related Rocks*, vol. 1, *Their Composition, Occurrence, Origin, and Emplacement*, edited by J. Ross, *Geol. Soc. Aust. Spec. Publ.*, 14, 358–368.

Hyndman, R. D. (1988), Dipping seismic reflectors, electrically conductive zones and trapped water in the crust over a subducting plate, *J. Geophys. Res.*, *93*, 13,391–13,405.

Irving, E., and P. J. Wynne (1991), Paleomagnetic evidence for motions of parts of the Canadian Cordillera, *Tectonophysics*, *187*, 259–275.

Johnston, S. T., P. J. Wynne, D. Francis, C. J. R. Hart, R. J. Enkin, and D. C. Engebretson (1996), Yellowstone in Yukon: The late Cretaceous Carmacks group, *Geology*, *25*, 42–44.

Jones, A. G. (1983), The problem of "current channelling": A critical review, *Geophys. Surv.*, *6*, 79–122.

Jones, A. G. (1987), MT and reflection: An essential combination, *Geophys. J.R. Astron. Soc.*, *89*, 7–18.

Jones, A. G. (1988), Static shift of magnetotelluric data and its removal in a sedimentary basin environment, *Geophysics*, *53*, 967–978.

Jones, A. G. (1992), Electrical conductivity of the continental lower crust, in *Continental Lower Crust*, edited by D. M. Fountain, R. J. Arculus, and R. W. Kay, pp. 81–143, Elsevier Sci., New York.

Jones, A. G., and D. I. Gough (1995), Electromagnetic studies in southern and central Canadian Cordillera, *Can. J. Earth Sci.*, *3*, 1541–1563.

Jones, A. G., A. D. Chave, G. Egbert, D. Auld, and K. Bahr (1989), A comparison of techniques for magnetotelluric response function estimation, *J. Geophys. Res.*, *94*, 14,201–14,213.

Jones, A. G., I. J. Ferguson, A. D. Chave, R. L. Evans, and G. W. McNeice (2001), The electric lithosphere of the Slave craton, *Geology*, *29*, 423–426.

Karato, S. (1990), The role of hydrogen in the electrical conductivity of upper mantle, *Nature*, *347*, 272–273.

Kurtz, R. D., J. M. DeLaurier, and J. C. Gupta (1986), A magnetotelluric sounding across Vancouver islands detect the subducting Juan de Fuca Plate, *Nature*, *325*, 596–599.

Kurtz, R. D., J. M. DeLaurier, and J. C. Gupta (1990), The electrical conductivity distribution beneath Vancouver Island: A region of active plate subduction, *J. Geophys. Res.*, *95*, 10,929–10,946.

Ledo, J., and A. G. Jones (2001), Regional electrical resistivity structure of the southern Canadian Cordillera and its physical interpretation, *J. Geophys. Res.*, *106*, 30,755–30,769.

Ledo, J., A. G. Jones, I. J. Ferguson, and G. Wennberg (2002a), SNORCLE corridor 3 magnetotelluric experiment, in *SNORCLE Trancset and Cordilleran Tectonics Workshop Meeting*, compiled by F. Cook and P. Erdmer, *Lithoprobe Rep. 82*, pp. 21–24, Univ. of B. C., Lithoprobe Secr. for the Can. Lithoprobe Program, Vancouver.

Ledo, J., A. G. Jones, and I. J. Ferguson (2002b), Electromagnetic images of a strike-slip fault: The Tintina fault—Northern Canadian, *Geophys. Res. Lett.*, *29*(8), 1225, doi:10.1029/2001GL013408.

Lewis, T., R. D. Hyndman, and P. Flück (2002), Thermal controls on present tectonics in northern canadian Cordillera: Snorcle, in *SNORCLE Trancset and Cordilleran Tectonics Workshop Meeting*, compiled by F. Cook and P. Erdmer, *Lithoprobe Rep. 82*, pp. 15–16, Univ. of B. C., Lithoprobe Secr. for the Can. Lithoprobe Program, Vancouver.

Lowe, C., R. B. Horner, J. K. Mortensen, S. T. Johnston, and C. F. Roots (1994), New geophysical data from the northern Cordillera: Preliminary interpretations and implications for the tectonics and deep geology, *Can. J. Earth Sci.*, *31*, 891–904.

Mackie, R., S. Rieven, and W. Rodi (1997), Users manual and software documentation for two-dimensional inversion of magnetotelluric data, GSY-USA, Inc., San Francisco, Calif.

Mathez, E. A., A. G. Duba, C. L. Peach, A. Léger, T. J. Shankland, and G. Plafker (1995), Electrical conductivity and carbon in metamorphic rocks of the Yukon-Tanana terrane, Alaska, *J. Geophys. Res.*, *100*, 10,187–10,196.

Mazzotti, S., and R. D. Hyndman (2002), Yakutat collision and stress transfer across the northern Canadian Cordillera, *Geology*, *30*, 495–498.

McNeice, G., and A. G. Jones (2001), Multi-site, multi-frequency tensor decomposition of magnetotelluric data, *Geophysics*, *66*, 158–173.

Monger, J. W. H. (1989), Overview of Cordilleran Geology, in *Western Canada Sedimentary Basin: A Case History*, edited by B. D. Ricketts, *Spec. Publ. 30*, pp. 9–32, Can. Soc. of Pet. Geol., Calgary, Alberta.

Monger, J. W. H., and R. Price (2002), The Canadian Cordillera: Geology and tectonic evolution, *CSEG Recorder*, *27*, 17–36.

Monger, J. W. H., et al. (1985), *Continent-Ocean Transect B2, Juan de Fuca Plate to Alberta Plains*, *Centennial Continent/Ocean Transect 7*, Geol. Soc. of Am., Boulder, Colo.

Morris, G. A., and R. A. Creaser (1998), The petrogenesis of the Mount Skukum/Bennett lake igneous complex, Yukon territory, and reflections on the Eocene tectonics of the Canadian Cordillera, in *SNORCLE Trancset and Cordilleran Tectonics Workshop Meeting*, compiled by F. Cook and P. Erdmer, *Lithoprobe Rep. 64*, pp. 165–170, Univ. of B. C., Lithoprobe Secr. for the Can. Lithoprobe Program, Vancouver.

Olhoeft, G. R. (1981), Electrical properties of granite with implications for the lower crust, *J. Geophys. Res.*, *86*, 931–936.

Oliver, D. H., V. L. Hansen, M. de Keijzer, P. F. Williams, and R. L. Brown (2001), Kilometre-scale folding in the Teslin Zone, northern Canadian Cordillera, and its tectonic implications for the accretion of the Yukon-Tanana Terrane to North America: Discussion and reply, *Can. J. Earth Sci.*, *38*, 879–887.

Page, R. A., G. Plafker, G. S. Fuis, W. J. Nokleberg, E. L. Ambos, W. D. Mooney, and D. L. Campbell (1986), Accretion and subduction tectonics in the Chugach Mountains and Cooper River Basin, Alaska: Initial results of the Trans-Alaska Crustal Transect, *Geology*, *14*, 501–505.

Park, S. K., and R. L. Mackie (1997), Crustal structure at Nanga Parbat, northern Pakistan, from magnetotelluric soundings, *Geophys. Res. Lett.*, *24*, 2415–2418.

Parrish, R. R., S. D. Carr, and L. Parkinson (1988), Eocene extensional tectonics and geochronology of the southern Omineca Belt, British Columbia and Washington, *Tectonics*, *7*, 181–212.

Peacock, S. M. (1996), Thermal and petrological structure of subduction zones, in *Subduction, Top to Bottom*, *Geophys. Monogr. Ser.*, vol. 96, edited by G. E. Bebout et al., pp. 119–133, AGU, Washington, D. C.

Rodi, W., and R. L. Mackie (2001), Nonlinear conjugate gradients algorithm for 2–D magnetotelluric inversion, *Geophysics*, *66*, 174–187.

Schwalenberg, K., V. Rath, and V. Haak (2002), Sensitivity studies applied to a 2–D resistivity model for the central Andes, *Geophys. J. Int.*, *150*, 673–686.

Shankland, T. J., and M. E. Ander (1983), Electrical conductivity, temperatures, and fluids in the lower crust, *J. Geophys. Res.*, *88*, 9475–9484.

Shi, L., D. Francis, J. Ludden, A. Frederiksen, and M. Bostock (1998), Xenolith evidence for lithospheric melting above anomalously hot mantle under the northern Canadian Cordillera, *Contrib. Mineral Petrol.*, *131*, 39–53.

Snyder, D., and B. Roberts (2001), Seismic characterization of two major tectonic zones in the Canadian Cordillera: The Teslin and Tintina zones along SNORCLE Line 3, in *SNORCLE Transect and Cordilleran Tectonics Workshop Meeting*, *Lithoprobe Rep. 79*, compiled by F. Cook and P. Erdmer, pp. 50–53, Univ. of B. C., Lithoprobe Secr. for the Can. Lithoprobe Program, Vancouver.

Snyder, D. B., R. M. Clowes, F. A. Cook, P. Erdemer, C. A. Evenchik, A. J. van der Velen, and K. W. Hall (2002), Proterozoic prism arrests suspect terranes: Insights into the ancient cordilleran margin from seismic reflection data, *GSA Today*, *12*, 4–10.

Stanley, W. D., V. F. Labson, W. J. Nokleberg, B. Csejtey, and M. A. Fisher (1990), The Denali fault system and Alaska Range of Alaska: Evidence for underplated Mesozoic flysch from magnetotelluric surveys, *Geol. Soc. Am. Bull.*, *102*, 160–173.

Stevens, R. A., and P. Erdmer (1996), Structural divergence and transpression in the Teslin tectonic zone, southern Yukon Territory, *Tectonics*, *15*, 1342–1363.

Swift, C. M. (1967), A magnetotelluric investigation of an electrical conductivity anomaly in the south western United States, Ph.D. thesis, Mass. Inst. of Technol., Cambridge.

Tempelman-Kluit, D. J. (1979), Transported cataclasite, ophiolite, and granodiorite in Yukon: Evidence of arc-continent collision, *Pap. Geol. Surv. Can.*, *79-14*, 27 pp.

Thorkelson, D. J. (1996), Subduction of diverging plates and the principles of slab window formation, *Tectonophysics*, *255*, 47–63.

Thorkelson, D. J., and R. P. Taylor (1989), Cordilleran Slab windows, *Geology*, *7*, 833–866.

Vozoff, K. (1991), The magnetotelluric method, in *Electromagnetic Methods in Applied Geophysics—Applications*, pp. 641–712, Soc. of Explor. Geophys., Tulsa, Okla.

Wannamaker, P. E., G. W. Hohmann, and S. H. Ward (1984), Magnetotelluric responses of three-dimensional bodies in layered earths, *Geophysics*, *49*, 1517–1533.

Wannamaker, P. E., J. R. Booker, A. G. Jones, A. D. Chave, J. H. Filloux, H. S. Waff, and L. K. Law (1989), Resistivity cross section through the Juan de Fuca subduction system and its tectonic implications, *J. Geophys. Res.*, *94*, 14,127–14,144.

Welford, J. K., R. M. Clowes, R. M. Ellis, G. D. Spence, I. Asudeh, and Z. Hajnal (2001), Lithospheric structure across the craton-Cordilleran transition of northeastern British Columbia, *Can. J. Earth Sci.*, *38*, 1169–1189.

Wennberg, G. (2003), Magnetotelluric response of the northern Cordillera: Interpretation of the lithospheric structure of the SNORCLE Transect, Corridor 2, M.Sc. thesis, Univ. of Manitoba, Winnipeg.

Wennberg, G., I. J. Ferguson, J. Ledo, and A. G. Jones (2002), Modeling and interpretation of magnetotelluric data: Watson Lake to Stewart (line2A) and Johnsons's Crossing to Watson lake, in *SNORCLE Trancset and Cordilleran Tectonics Workshop Meeting*, compiled by F. Cook and P. Erdmer, *Lithoprobe Rep. 82*, p. 145, Univ. of B. C., Lithoprobe Secr. for the Can. Lithoprobe Program, Vancouver.

Xu, Y., and T. J. Shankland (1999), Electrical conductivity of orthopyroxene and its high pressure phases, *Geophys. Res. Lett.*, *26*, 2645–2648.

Xu, Y., T. J. Shankland, and B. T. Poe (2000), Laboratory-based electrical conductivity of the Earth's mantle, *J. Geophys. Res.*, *105*, 27,865–27,875.

I. J. Ferguson and L. Wolynec, Geological Sciences, University of Manitoba, Winnipeg, Manitoba, Canada R3T 2N2.

A. G. Jones, Dublin Institute for Advanced Studies, 5 Merrion Square, Dublin 2, Ireland. (alan@cp.dias.ie)

J. Ledo, Departament de Geodinamica i Geofisica, Universitat de Barcelona, Barcelona, E-08013 Spain. (jledo@ub.edu)